

Research Article

CFD Analysis of NACA 0012 Aerofoil to Investigate the Effect of Increasing Angle of Attack on Coefficient of Lift and Coefficient of Drag

Mirza Haseeb Khalid ^{1,*} 

¹ Department of Mechanical Engineering, University of Engineering and Technology Lahore, Lahore, 54000, Pakistan

*Corresponding Author: Mirza Haseeb Khalid, E-mail: engr.mhaseebk@gmail.com

Article Info	Abstract
Article History	The significance of using proper blade design is increasing with advancements in aviation technology. Wings are used in a variety of applications, including aircraft, drones, wind turbines, and more. In this study, Ansys version 2021 is used to do a CFD analysis on a NACA 0012 to study the effect of increasing the angle of attack on the coefficient of lift. Analyses have been performed using Ansys Fluent. The k-w turbulence model was used to analyze geometry, designed in SOLIDWORKS. At a speed of 32 m/s, several angles of attack have been evaluated from 0° to 20° to investigate lift and drag coefficient. The results of this study were compared with the literature for validation. It has been observed that increasing the angle of attack will increase the lift coefficient initially but after a specific angle, flow separation takes place and the lift coefficient starts decreasing with a further increase in the angle of attack.
Received Feb 26, 2022	
Revised Mar 28, 2022	
Accepted Mar 31, 2022	
Keywords	
Fluid Dynamics	
NACA	
Aerofoil	
Aerodynamics	



Copyright: © 2022 Mirza Haseeb Khalid. This article is an open-access article distributed under the terms and conditions of the Creative Commons Attribution (CC BY 4.0) license.

1. Introduction

In the recent decade, the application of Computational Fluid Dynamics (CFD) in aviation has aided in the understanding of fluid dynamics and aero processes[1]. Additionally, numerical simulations have proven themselves as a key and ever-evolving component of the aircraft design process. CFD reduces the dependency on experimental investigations through wind tunnels, lowering design costs in the process. As a result of these advancements, wing performance is improved through the use of CFD technologies[1, 2].

Wings are designed and developed to achieve the maximum lift for an airplane. Nearly all commercial jets and propeller-driven planes have an aerodynamic component known as an airfoil. Using an airfoil profile, the wings of an airplane can generate more lift, reducing the amount of energy required for flight[3]. Lift is one of the active forces that permit airplanes to move from one location to another, alongside propulsion. Propulsion is provided by an airplane's engine or engines, while the lift is provided by the wings and body of the aircraft[4]. Airplanes with wings in the shape of an airfoil provide greater lift than those

with wings in a different shape[5]. As a result, they can stay in the air for longer periods. As a result, fluid flows at varying speeds across the surface of the geometry of aerofoil [6].

Figure 1 is a schematic diagram indicating the aerofoil geometry which is a major component in providing necessary lift to airplanes. When an aerofoil is moved at a particular speed, it generates aerodynamic forces (lift and drag)[7]. Drag force acts in the opposite direction of motion while the force that is in the vertical direction provides lift. Lift Force is created by the difference in pressures on top and bottom surfaces. Air travels at the same speed across both the top and bottom of an airplane's wings if they have the same shape. When an airplane's wings have an airfoil shape, air travels slower over the top than at the bottom. As a result, wings can generate extra lift because of the increased airflow. The curved airfoil design directs air downwards, resulting in a faster flow of air and thus more speed. Lift is increased in an airplane by the velocity differences between the top and bottom parts of the wing[8].

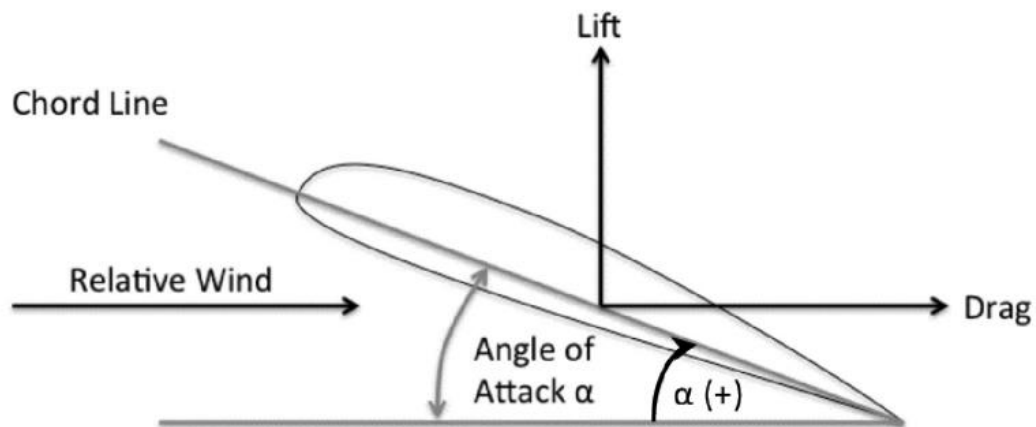


Figure 1. Aerofoil Schematic

The lift coefficient (C_L) is used to relate the lift of an aerofoil to the density of fluid that surrounds the geometry of the aerofoil. It is a dimensionless quantity[9].

$$C_L = \frac{L}{\frac{1}{2}\rho v^2 A} \quad (1)$$

Where, L represents the force of the lift, A represents aerofoil area, V represents air velocity, and ρ represents the density of air.

In fluid mechanics, resistance to an object placed in that fluid can be calculated using the coefficient of drag (C_D)[9, 10].

$$C_D = \frac{D}{\frac{1}{2}\rho v^2 A} \quad (2)$$

Where, D represents the force of drag, A represents aerofoil area, V represents air velocity, and ρ represents the density of air.

NACA aerofoils are aerofoils that have been standardized by the National Advisory Committee for Aeronautics (NACA)[11]. They use special digits to indicate their geometries [12]. The Angle of Attack (AoA) is the angle formed by a construction line, used as a reference, on aerofoil body and vector that represents the relative motion between fluid and body that moves through it[13]. In the case of an airplane, the angle is defined as the angle between the direction of movement of the wing and the chord line of the wing. Each blade has its specific value of AoA for the highest value of lift. Laminar flow is converted to turbulent flow after a particular value of AoA. Turbulence has a direct impact on the amount of lift generated and reduces the coefficient of lift[14].

In this study, SOLIDWORKS will be used to generate the geometry of NACA 0012 aerofoil and the fluid domain. Ansys Fluent will be used to study the relationship between the different angles of attacks and the coefficient of lift.

2. Materials and Methods

NACA 0012 profile was created in SOLIDWORKS. After the generation of geometry, a fluid domain of the profile was generated. The fluid domain was then imported into Ansys Fluent for CFD simulations. K- ω turbulence model was selected to conduct this study. Different cases, with different components of inlet velocities, were generated to study the effect of changing the angle of attack.

2.1. Geometry Creation using SOLIDWORKS

The curve data points were imported into SOLIDWORKS and the top and bottom curves of the aerofoil were created. Following that, a fluid domain was formed around it. Two fluid domains were created, one near the aerofoil and one away from it. This was done to increase the mesh quality near critical regions. After successful generation of the fluid domain, the model was saved in the '.step' format for import into Ansys Fluent. Figure 2 shows the final geometry and Figure 3 show the dimensional details of the domain.

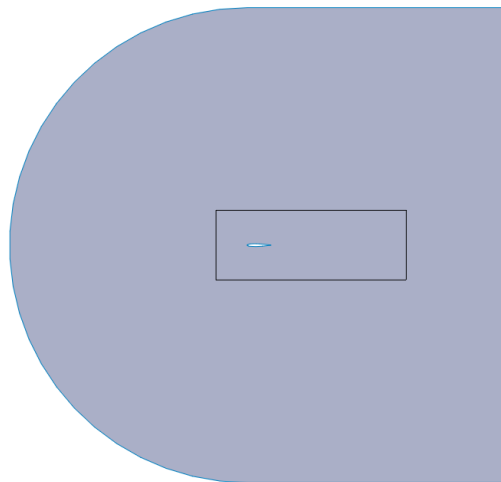


Figure 2. Fluid domain generation using SOLIDWORKS

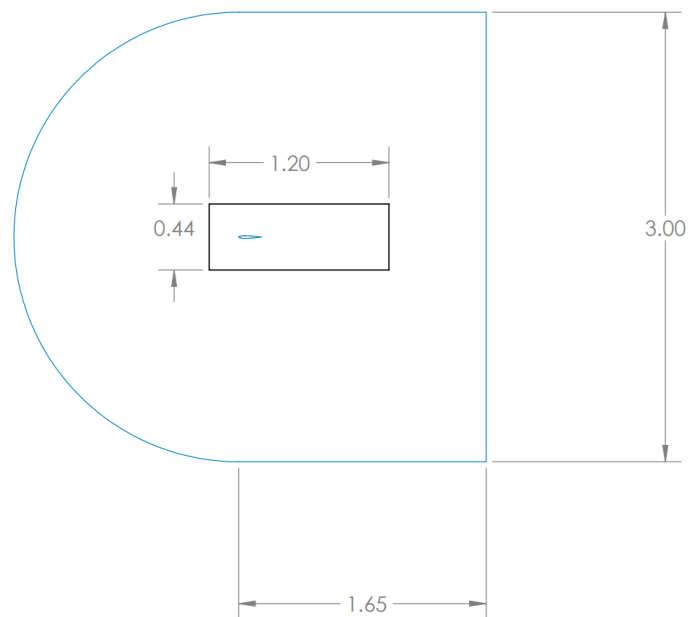


Figure 3. Dimensional details of the fluid domain

2.3 Computational Fluid Dynamics (CFD)

After finalizing the geometry, the Ansys workbench was run and geometry was imported in Fluent. Using Ansys Mechanical, a mesh was generated. Several mesh refinements were applied during mesh generation including body sizing, inflation, and method. Special attention was given to mesh size near to edges of an aerofoil. Figure 4 represents the final mesh generated for this analysis. Figure 5 represents mesh near aerofoil.

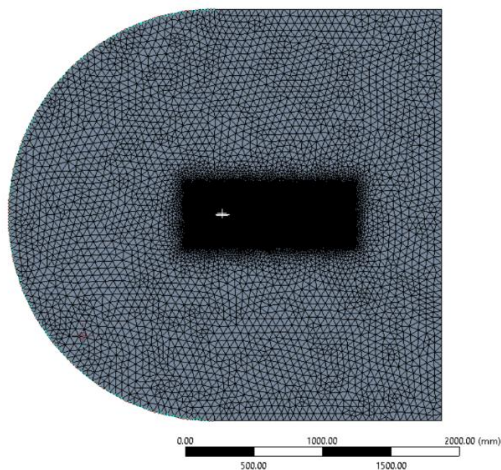


Figure 4. Created fluid domain and mesh generation

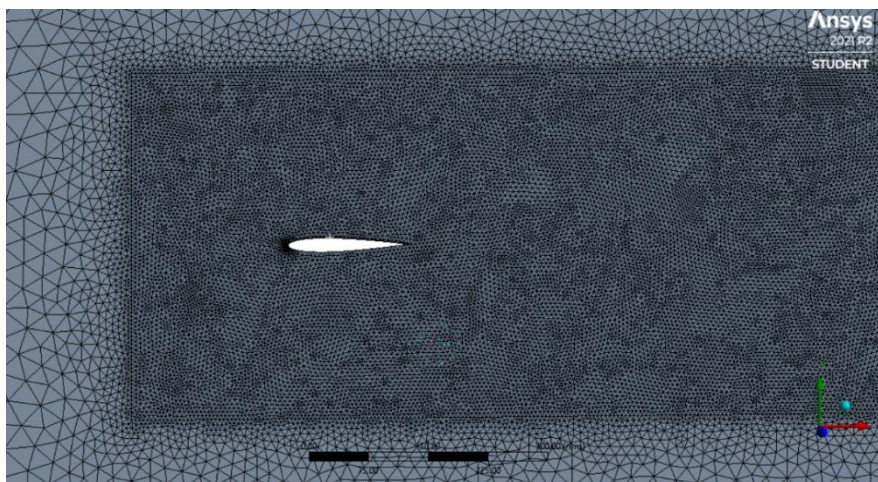


Figure 5. Distribution of mesh around an aerofoil

Named selection is one of the most important steps while conducting a CFD analysis because it makes it easier to set the boundary conditions. In this study, several named selections were used and details of each named selection are shown in Figure 6.

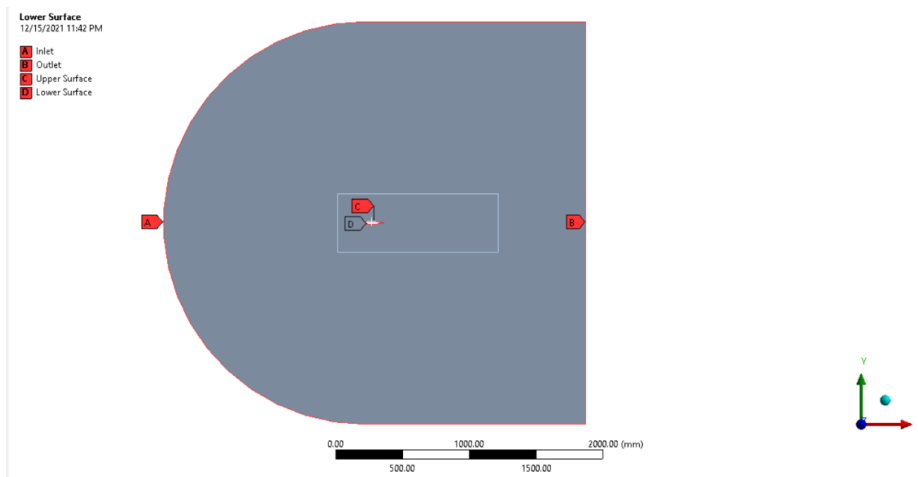


Figure 6. Named selections

After named selection and meshing, Ansys mechanical is closed and fluent is run. As in this case, different angles of attack are to be analyzed, it is important to find the horizontal and vertical components of velocity at each angle of attack. Figure 8 indicates the input velocity of 32 m/s for 0 angles of attack. Table 1. shows the horizontal and vertical components of velocities at different angle of attacks from 0° to 20°.

Table 1. The horizontal and vertical components of velocities

Angle of attack	X value	Y value	Velocity x	Velocity y
1	0.9998	0.017	31.9936	0.544
2	0.9993	0.0348	31.9776	1.1136
3	0.998	0.052	31.936	1.664
4	0.997	0.069	31.904	2.208
5	0.996	0.087	31.872	2.784
6	0.994	0.104	31.808	3.328
7	0.9925	0.121	31.76	3.872
8	0.99	0.139	31.68	4.448
9	0.987	0.156	31.584	4.992
10	0.984	0.1736	31.488	5.5552
11	0.981	0.19	31.392	6.08
12	0.978	0.207	31.296	6.624
13	0.974	0.225	31.168	7.2
14	0.97	0.24	31.04	7.68
15	0.965	0.258	30.88	8.256
16	0.961	0.275	30.752	8.8
17	0.956	0.292	30.592	9.344
18	0.951	0.309	30.432	9.888
19	0.945	0.325	30.24	10.4
20	0.939	0.342	30.048	10.944

Ansys has a variety of turbulence models. While doing the literature study, it was observed that the k- ω model was widely used. Additionally, it is recommended in applications for cases with low Reynolds Numbers. The aerodynamic performance of NACA 0012 was determined through simulations. Figure 7. indicates the reference values used in this simulation.

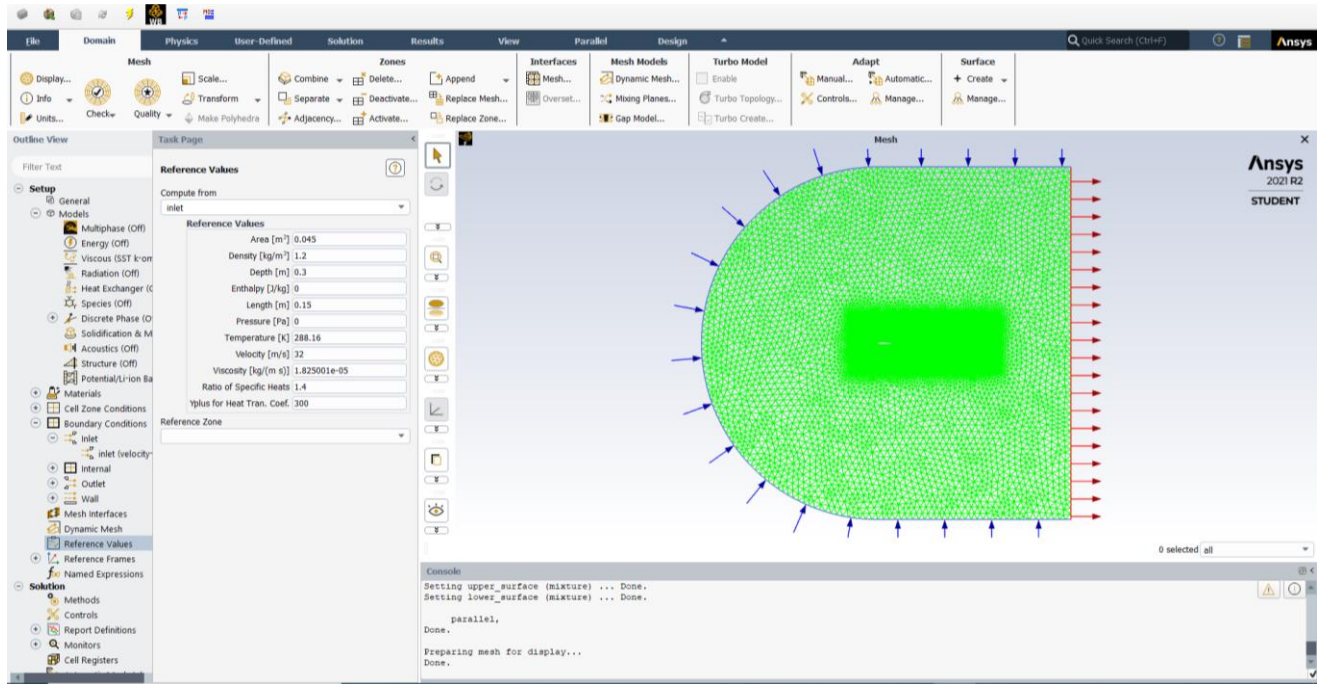


Figure 7. Reference values detail

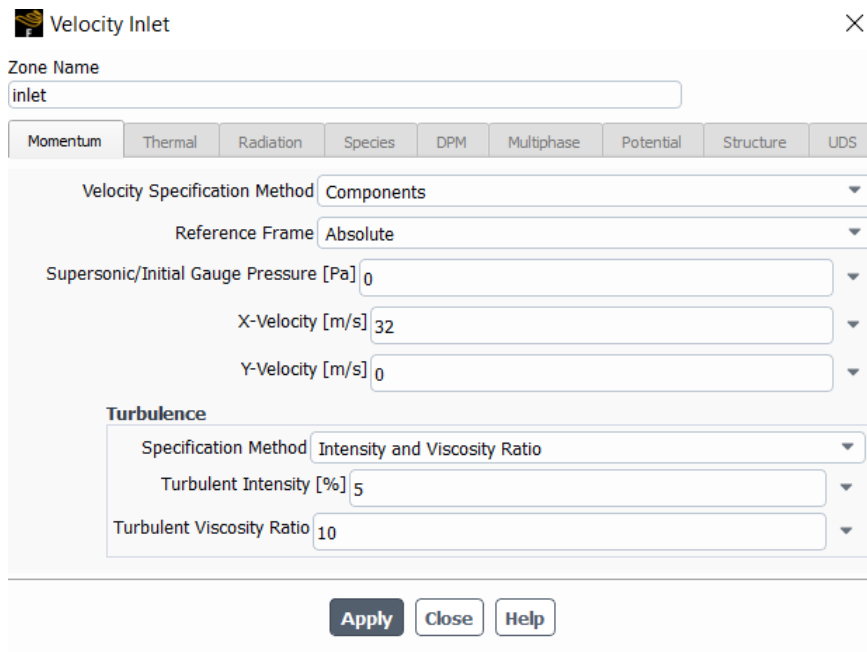


Figure 8. Input velocity at 0° AoA

3. Results and Discussions

3.1 Velocity Contours

The contours of velocity magnitude produced from CFD simulations for various angles of attack are illustrated in Figures 9, 10, 11, 12, 13, 14, and 15. Stagnation point occurs on the leading edge resulting in zero velocity.

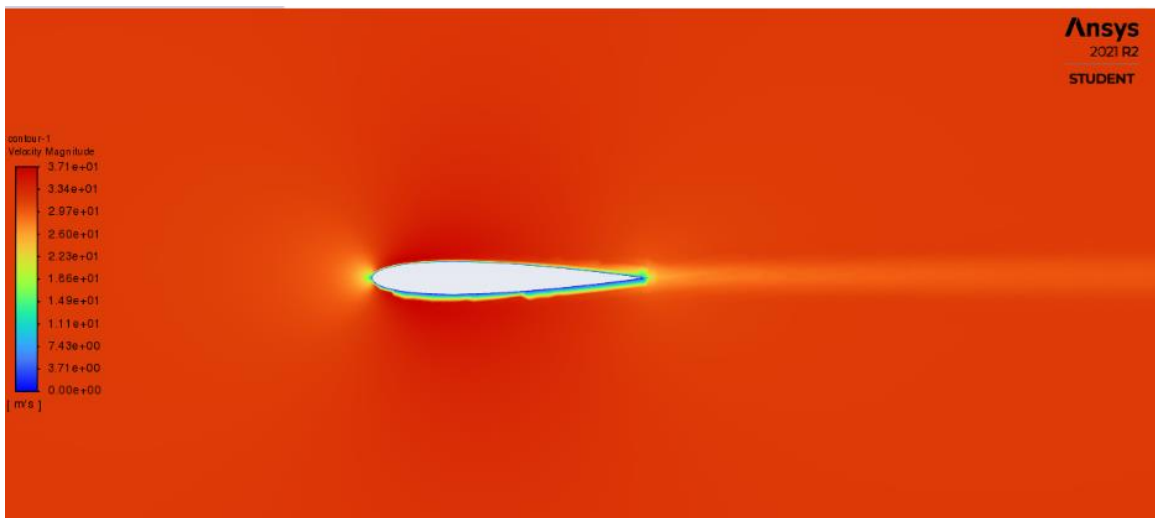


Figure 9. Velocity contour at 0 degrees AoA

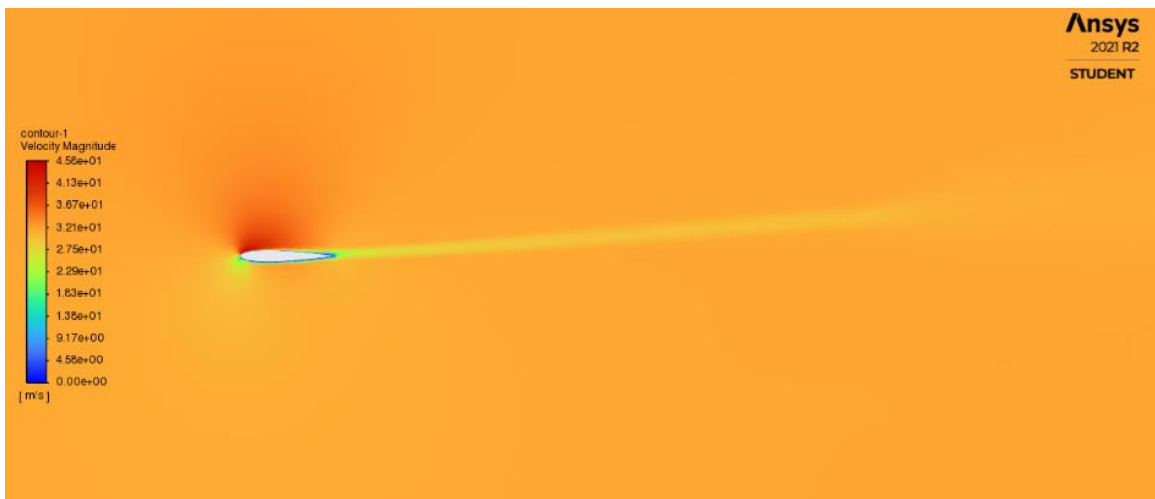


Figure 10. Velocity contour at 5 degrees AoA

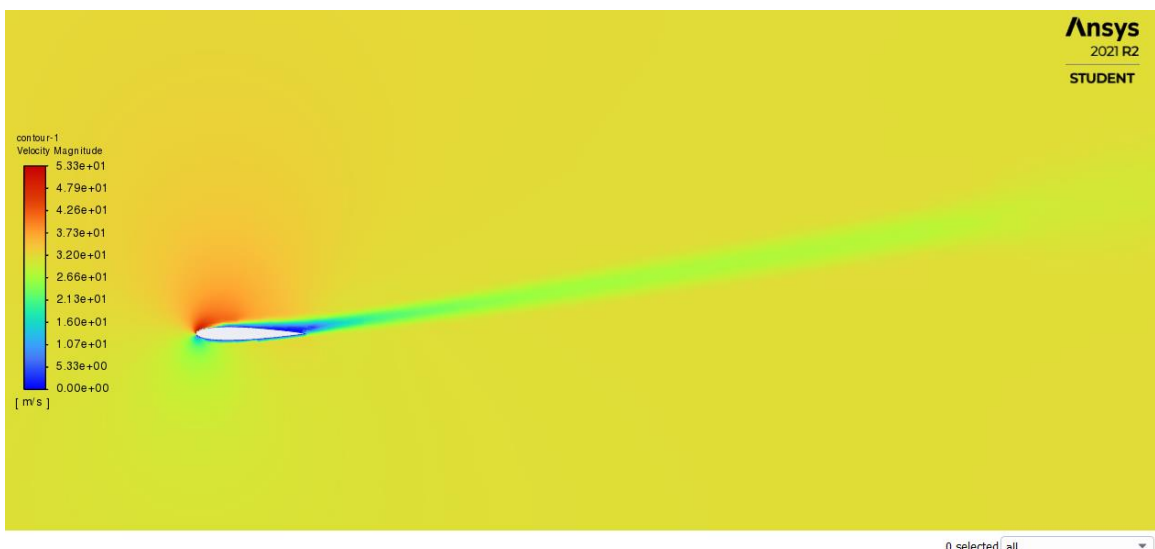


Figure 11. Velocity contour at 10 degrees AoA

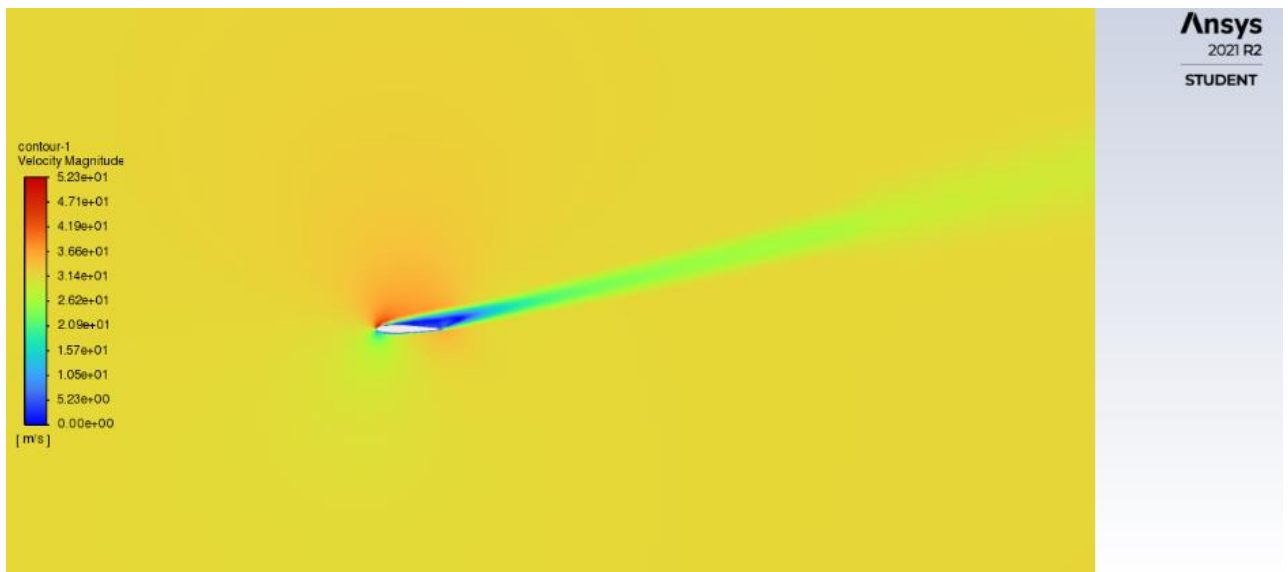


Figure 12. Velocity contour at 15 degrees AoA



Figure 13. Velocity contour at 20 degrees AoA

3.2. Pressure Contours

The contours of pressure magnitude generated from CFD simulations for various angles of attack are presented in Figures 14, 15, 16, 17, and 18. According to the application of Bernoulli's principle, when the velocity is high, pressure is low. The same applies here, in the top region, the pressure is low because of increased velocity, and as a result, high pressure on the bottom pushes the geometry upward creating the lift force.

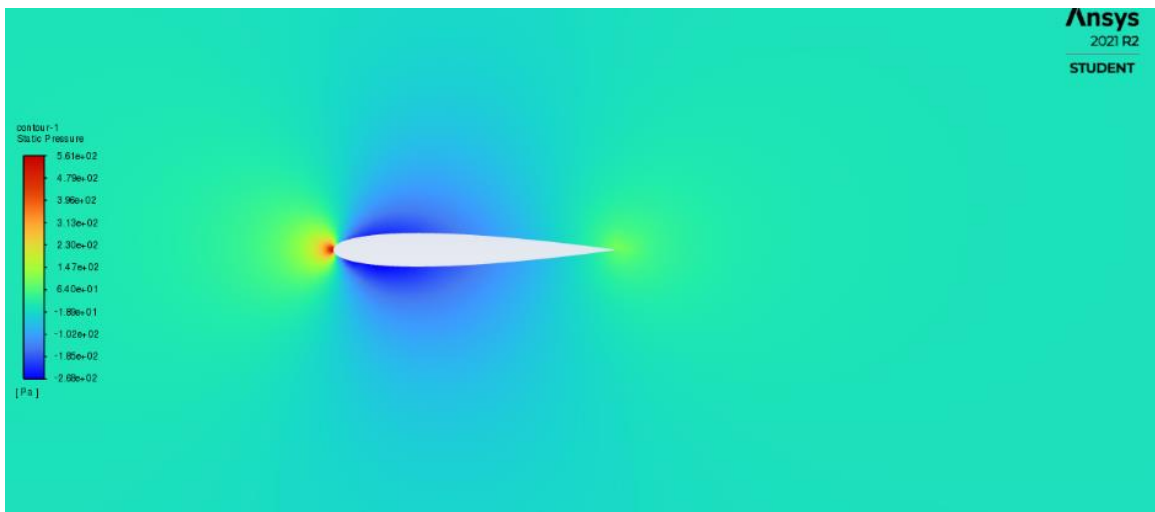


Figure 14. Pressure contour at 0 degrees AoA

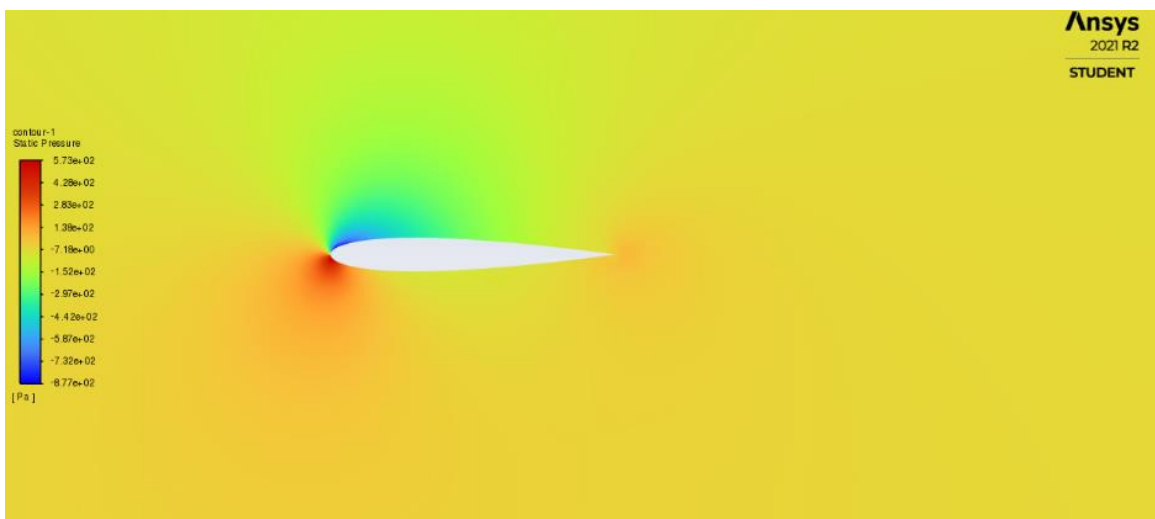


Figure 15. Pressure contour at 5 degrees AoA



Figure 16. Pressure contour at 10 degrees AoA

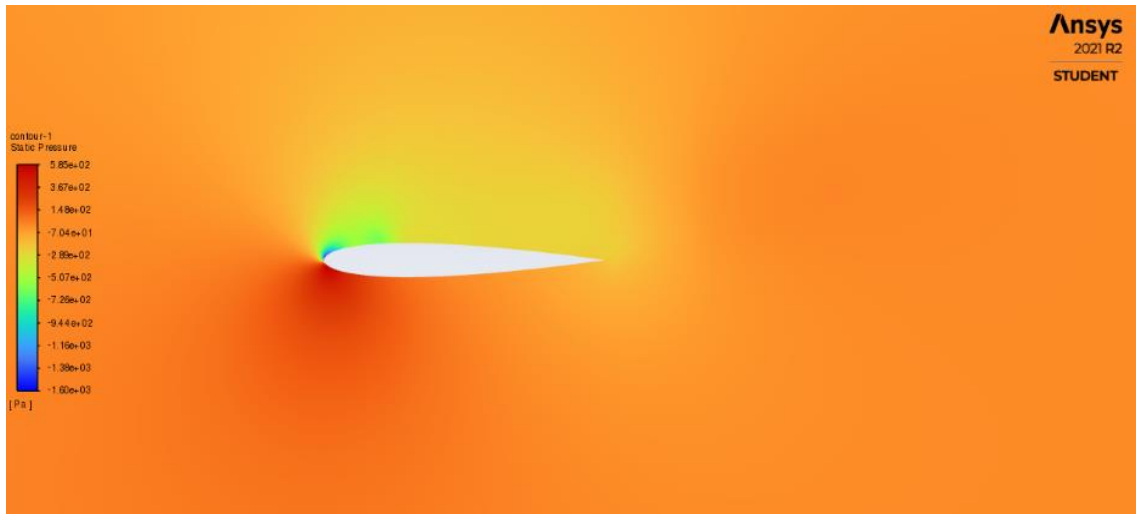


Figure 17. Pressure contour at 15 degrees AoA

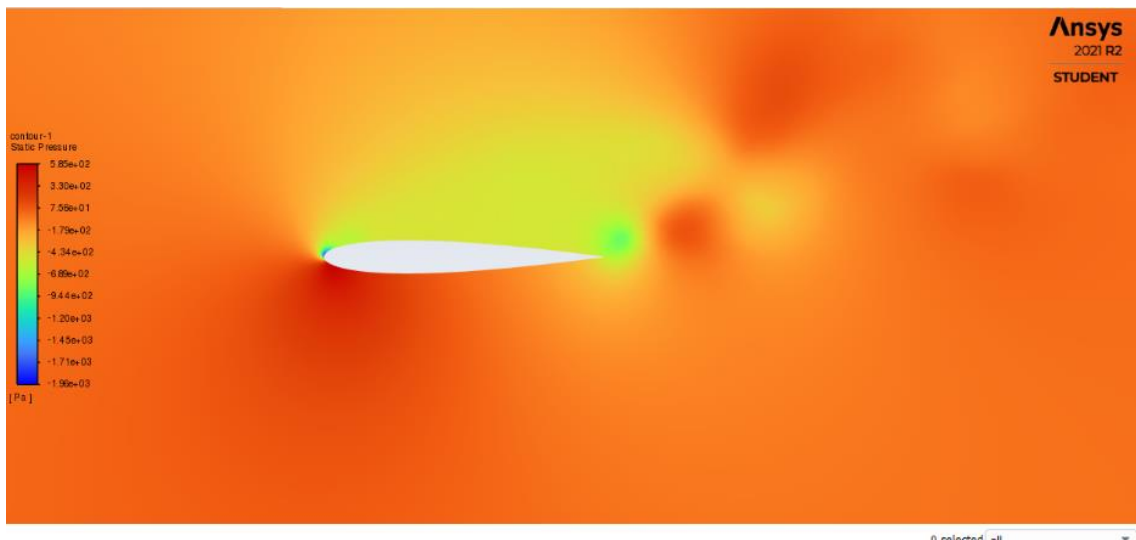


Figure 18. Pressure contour at 20 degrees AoA

3.3. Graph of Lift Coefficient

Figure 19 shows the calculated lift coefficients at an angle of attacks ranging from 0° to 20° . It can be inferred from the graph that with an increase in the angle of attack, C_L increases as well. But after 14° , further increase in the angle of attack reduces the C_L . Due to the high value of the pressure gradient, pressure forces overcome the inertial forces of fluid, and separation of fluid takes place. This fluid separation is responsible for the decrease in the C_L with further increase in AoA.

3.4. Comparison with Literature

Figure 20 shows the comparison of simulation results with the experimental results. In this figure, the results of the lift coefficient are indicated on the graph. The curve with 'measured' results indicates the

results obtained from the literature[15]. The experimental results validate the results obtained from the simulation in this study.

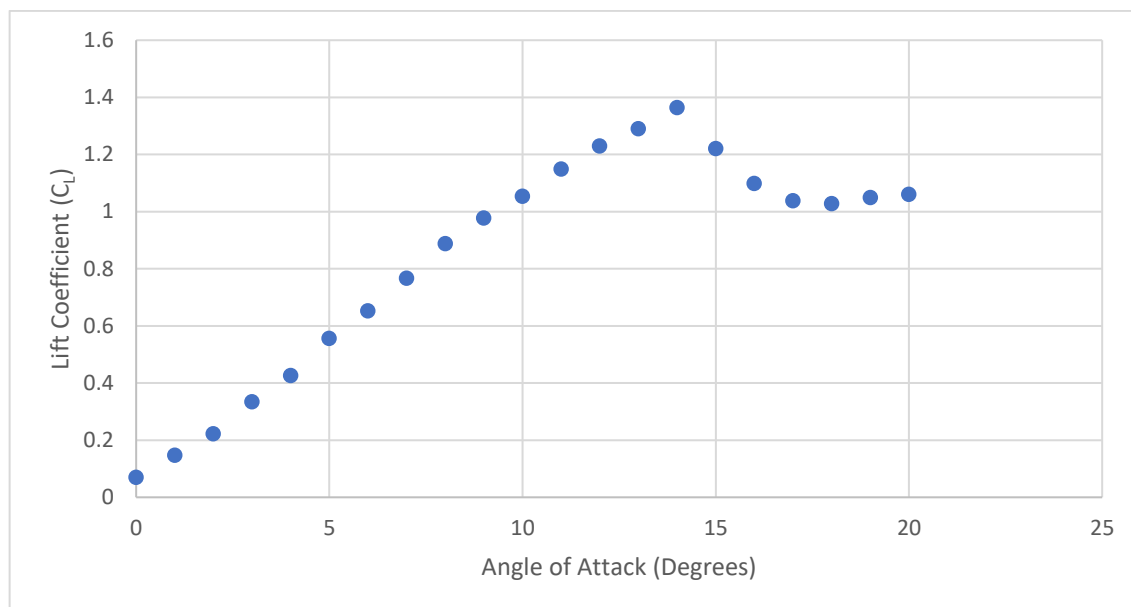


Figure 19. Calculated lift coefficient values at different angles of attack

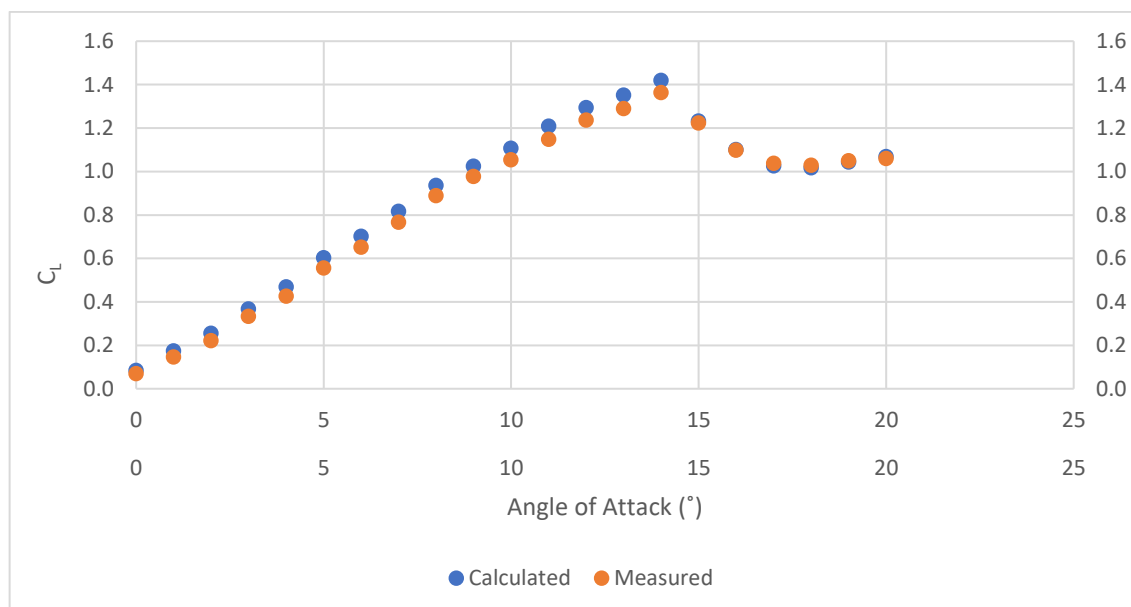


Figure 20. Comparison of calculated lift coefficients with literature

4. Conclusions

In this study, NACA0012 airfoil aerodynamic performance was studied using CFD software Ansys Fluent at various angles of attack from 0 degrees to 20 degrees with a constant velocity of 32 m/s. Contours of velocities and pressures were presented to study the flow around the Aerofoil. Using Fluent, C_L was

evaluated for all angles of attacks. A graph was plotted for calculated C_L against AoA. The trend of the graph suggested that with an increase in the angle of attack, C_L increases as well until flow separation takes place C_L starts decreasing with further increase in AoA. Validation of the calculated results was done by comparing the results with the literature.

Declaration of Competing Interest: The author declares no conflict of interest.

References

- [1] K. S. Patel, S. B. Patel, U. B. Patel, and A. P. Ahuja, "CFD Analysis of an Aerofoil," *International Journal of Engineering Research*, vol. 3, no. 3, pp. 154-158, 2014.
- [2] M. F. Ismail and K. Vijayaraghavan, "The effects of aerofoil profile modification on a vertical axis wind turbine performance," *Energy*, vol. 80, pp. 20-31, 2015.
- [3] F. Dehaeze, G. Barakos, A. Batrakov, A. Kusyumov, and S. Mikhailov, "Simulation of flow around aerofoil with DES model of turbulence," *Труды МАИ*, no. 59, 2012.
- [4] M. YILMAZ, H. KÖTEN, E. Çetinkaya, and Z. Coşar, "A comparative CFD analysis of NACA0012 and NACA4412 airfoils," *Journal of Energy Systems*, vol. 2, no. 4, pp. 145-159, 2018.
- [5] S. K. Rasal and R. R. Katwate, "Numerical analysis of lift & drag performance of NACA0012 wind turbine aerofoil," *International Research Journal of Engineering and Technology*, vol. 4, no. 06, pp. 2892-2896, 2017.
- [6] F. M. White, *Fluid mechanics*. Tata McGraw-Hill Education, 1979.
- [7] S. J. Juliyana, J. U. Prakash, K. Karthik, P. Pallavi, and M. Saleem, "Design and analysis of NACA4420 wind turbine aerofoil using CFD," *International Journal of Mechanical Engineering and Technology*, vol. 8, no. 6, pp. 403-410, 2017.
- [8] K. S. Rao, M. A. Chakravarthy, G. S. Babu, and M. Rajesh, "MODELING AND SIMULATION OF AEROFOIL ELEMENT," *METHODOLOGY*, vol. 5, no. 02, 2018.
- [9] T. Liu, S. Wang, X. Zhang, and G. He, "Unsteady thin-airfoil theory revisited: application of a simple lift formula," *Aiaa Journal*, vol. 53, no. 6, pp. 1492-1502, 2015.
- [10] H. Yang, M. Fan, A. Liu, and L. Dong, "General formulas for drag coefficient and settling velocity of sphere based on theoretical law," *International Journal of Mining Science and Technology*, vol. 25, no. 2, pp. 219-223, 2015.
- [11] M. S. A. Hakim *et al.*, "The effects of Reynolds number on flow separation of Naca Aerofoil," *Journal of Advanced Research in Fluid Mechanics and Thermal Sciences*, vol. 47, no. 1, pp. 56-68, 2018.
- [12] N. Eastman, E. Kenneth, and R. Pinkerton, "The characteristics of 78 related airfoil sections from tests in the variable-density wind tunnel," *NACA-report-460*, 1933.
- [13] T. A. Johansen, A. Cristofaro, K. Sørensen, J. M. Hansen, and T. I. Fossen, "On estimation of wind velocity, angle-of-attack and sideslip angle of small UAVs using standard sensors," in *2015 International Conference on Unmanned Aircraft Systems (ICUAS)*, 2015: IEEE, pp. 510-519.
- [14] D. Barkley, B. Song, V. Mukund, G. Lemoult, M. Avila, and B. Hof, "The rise of fully turbulent flow," *Nature*, vol. 526, no. 7574, pp. 550-553, 2015.
- [15] S. Eftekhari and A. S. M. Al-Obaidi, "Investigation of a NACA0012 Finite Wing Aerodynamics at Low Reynold's Numbers and 0° to 90° Angle of Attack," *Journal of Aerospace Technology and Management*, vol. 11, 2019.